CHY Integrands from Factorization Channels and Exact Integer Propagation

Exact Constructions for Inverse Problems in Scattering Amplitudes

张曜勃

宁夏大学

2026 中国物理学会高能物理学术年会

Based on:
S. Li and Y. Zhang, *Phys. Rev. D* **113**, 105006 (2026);
L. Mai and Y. Zhang, arXiv:2607.13412 [hep-th] (2026).

Outline

1: Introduction

Scattering Amplitudes

For fixed initial and final states, the S-matrix is

$$S = \mathbf{1} + i(2\pi)^D \delta^{(D)}\left(\sum_i k_i\right) \mathcal{A}_n.$$

- $\mathcal{A}_n$ determines transition probabilities and cross sections;
- It encodes locality, unitarity, gauge invariance, and Lorentz invariance;
- Modern amplitude methods target its analytic and representation structure directly.

Source: D. Kosower et al., SAGEX Review on Scattering Amplitudes (2022).

Feynman Diagrams: The Standard Forward Calculation

Perturbative quantum field theory starts from a Lagrangian:

$$\text{Lagrangian} \longrightarrow \text{vertices and propagators} \longrightarrow \text{Feynman diagrams} \longrightarrow \mathcal{A}_n.$$

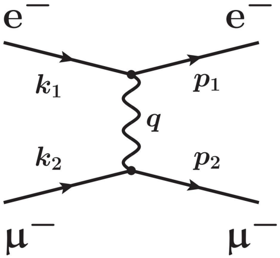

- Diagram counts grow rapidly with multiplicity and loop order;
- Individual diagrams are gauge dependent, while compact structures emerge only after summation.

Modern Amplitude Methods

The input data include

- factorization channels and pole structure;
- generalized unitarity cuts;
- soft, collinear, and multi-particle limits;
- gauge invariance, permutation symmetry, and Jacobi relations;
- locality and power counting.

physical data $\longrightarrow$ allowed representation space $\longrightarrow$ exact amplitude representation.

The Amplitude Bootstrap as an Inverse Problem

The amplitude bootstrap imposes physical constraints instead of summing diagrams:

$$\mathcal{D}_{\text{phys}} = \left\{ \begin{matrix} \text{factorization, generalized unitarity cuts, symmetries,} \\ \text{soft/collinear limits, locality} \end{matrix} \right\}.$$

Let C_α encode each condition. The goal is to determine the solution set

$$\mathcal{S}_{\text{boot}} = \{\mathcal{A} : \; C_\alpha[\mathcal{A}] = b_\alpha \text{ for all } \alpha\}.$$

- Physical data define an allowed solution set, not necessarily a unique formula;
- Different representations may encode the same amplitude;
- Physical limits not used in the construction provide held-out tests.

A Linear Inverse Problem

After choosing a basis, many amplitude constructions reduce to

$$\boxed{Ax = b}.$$

Here

- x: representation parameters;
- A: physical constraints compiled into linear measurements;
- b: target residues, cut data, or other physical readouts.

The solution set is the preimage, not a single point:

$$\mathcal{F}_b = \{x \in \mathcal{X} : \; Ax = b\}.$$

We must determine its existence, dimension, discrete branches, and physical equivalence relations.

Designing the Inverse Problem

At the first level, A and b are fixed:

$$(A, b) \text{ fixed} \qquad \Longrightarrow \qquad \mathcal{F}_b = \{x : Ax = b\}.$$

At the second level, a working specification σ also defines the operator:

$$\sigma \longrightarrow (A_\sigma, b_\sigma) \longrightarrow \mathcal{F}_\sigma \longrightarrow \text{held-out tests.}$$

If the system is inconsistent, underconstrained, or fails held-out tests, revise σ by changing the representation space or measurements.

$$\text{solve a fixed inverse problem} \qquad \longrightarrow \qquad \text{adaptively design the inverse problem.}$$

The two case studies illustrate these two levels.

2: Inverse CHY and Discrete Backpropagation

CHY Formula and Integrand

At tree level, the n-point amplitude is

$$\mathcal{A}_n = \int d\mu_n \mathcal{I}(z), \qquad d\mu_n = \frac{\prod_{i=1}^{n} dz_i}{\mathrm{vol}(\mathrm{SL}(2,\mathbb{C}))} \prod_a{}' \delta(\mathcal{E}_a),$$

$$\mathcal{E}_a = \sum_{b \neq a} \frac{s_{ab}}{z_a - z_b} = 0, \qquad s_{ab} = 2k_a \cdot k_b.$$

The measure is fixed by external kinematics; the CHY integrand $\mathcal{I}(z)$ encodes the theory. For example,

$$\mathrm{PT}(\alpha) = \frac{1}{z_{\alpha_1\alpha_2} \cdots z_{\alpha_n\alpha_1}}, \qquad \mathcal{I}_{\phi^3} = \mathrm{PT}(\alpha)\mathrm{PT}(\beta).$$

Each factor z_{ij}^{-1} is represented by an edge joining particles i and j.

Source: F. Cachazo, S. He and E. Y. Yuan, Phys. Rev. Lett. 113 (2014) 171601.

Graph Representation and Pole Index

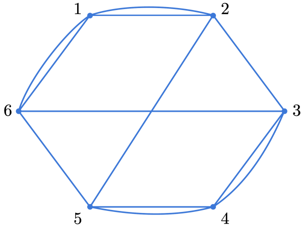

For a subset A of particle labels, let $L[A]$ count the edges internal to A. For a 4-regular integrand,

$$\boxed{\chi(A) = L[A] - 2(|A| - 1)}.$$

$$\chi(A) = 0: \ \text{candidate simple pole } \frac{1}{s_A}, \qquad \chi(A) < 0: \ \text{no pole}, \qquad s_A = \Big(\sum_{i \in A} k_i\Big)^2 = s_{\bar{A}}.$$

Each cubic term contains $n - 3$ mutually compatible simple poles.

Source: C. Baadsgaard et al., JHEP 09 (2015) 129.

Pole-Index Matrix

Let $\mathcal{E}$ be the edge set of the complete graph:

$$\mathcal{E} = \{(ij) : 1 \leq i < j \leq n\}, \qquad m = (m_{12}, m_{13}, \ldots, m_{n-1,n})^T \in \mathbb{Z}_{\geq 0}^{\binom{n}{2}}.$$

For each nontrivial subset A, define the binary subset–edge incidence matrix by

$$B_{A,(ij)} = \begin{cases} 1, & i, j \in A, \\ 0, & \text{otherwise.} \end{cases}$$

Then all channel pole indices are collected in

$$\boxed{\chi = Bm - r}, \qquad r_A = 2(|A| - 1).$$

If D is the vertex–edge incidence matrix, the 4-regularity condition is $Dm = 4\mathbf{1}$.

Source: S. Li and Y. Zhang, Phys. Rev. D 113, 105006 (2026).

Integer Constraints for Prescribed Poles

Prescribing target simple poles while excluding forbidden poles gives the integer system

$$\boxed{\begin{aligned} Dm &= 4\mathbf{1}, \\ B_{\rm tar}\, m &= r_{\rm tar}, \\ B_{\rm forb}\, m &\le r_{\rm forb} - \mathbf{1}, \qquad m \in \mathbb{Z}_{\ge 0}^{\binom{n}{2}}. \end{aligned}}$$

The number of variables is

$$N_{\rm var} = \binom{n}{2} = O(n^2).$$

After identifying $A \sim \bar{A}$, the number of channels to specify or check is

$$N_{\rm ch} = \frac{1}{2} \sum_{k=2}^{n-2} \binom{n}{k} = 2^{n-1} - n - 1 = O(2^n).$$

For $n = 6, 8, 10$, $(N_{\rm var}, N_{\rm ch}) = (15, 25), (28, 119), (45, 501)$.

Source: S. Li and Y. Zhang, Phys. Rev. D 113, 105006 (2026).

Generalized Pole Degree

For rational CHY integrands, define the generalized pole degree $K(A)$ as a signed internal-edge count:

$$K(A) = L_{\mathrm{solid}}[A] - L_{\mathrm{dashed}}[A] = \sum_{\substack{i<j \\ i,j\in A}} m_{ij}.$$

The pole index remains

$$\boxed{\chi(A) = K(A) - 2(|A| - 1)}.$$

Every prescribed pole constraint is therefore an integer equality or inequality:

$$K(A) = 2(|A| - 1) \quad \text{or} \quad K(A) \leq 2(|A| - 1) - 1.$$

An edge with $m_{ij} > 0$ is a solid denominator edge; one with $m_{ij} < 0$ is a dashed numerator edge. The subset recursion avoids treating every subset A independently.

Source: S. Li and Y. Zhang, Phys. Rev. D 113, 105006 (2026).

Subset Recursion for $K(A)$

For $|A| \geq 3$, each internal edge appears in $|A| - 2$ codimension-one subsets of A. Hence

$$\boxed{K(A) = \frac{1}{|A| - 2} \sum_{\substack{B \subset A \\ |B| = |A| - 1}} K(B)}.$$

For example,

$$K(123) = K(12) + K(13) + K(23),$$

$$K(1234) = \frac{1}{2}\big[K(123) + K(124) + K(134) + K(234)\big].$$

Data at each higher layer are determined recursively by the layer below.

Source: S. Li and Y. Zhang, Phys. Rev. D 113, 105006 (2026), Eq. (2.5).

Reduction to Two-Particle Data

Iterating the recursion down to the bottom layer gives

$$\boxed{K(A) = \sum_{\substack{i<j \\ i,j\in A}} K(ij)}.$$

Only the $\binom{n}{2}$ two-particle data $K(ij)$ are independent. Every higher-channel constraint becomes

$$\sum_{\substack{i<j \\ i,j\in A}} K(ij) \begin{cases} = 2(|A|-1), & A \in \mathcal{P}_{\mathrm{tar}}, \\ \leq 2(|A|-1)-1, & A \in \mathcal{P}_{\mathrm{forb}}. \end{cases}$$

This removes variables on higher layers and redundant interlayer equalities. Channels can still be generated and checked layer by layer.

Source: S. Li and Y. Zhang, Phys. Rev. D 113, 105006 (2026).

Subset Lattice of Pole Constraints

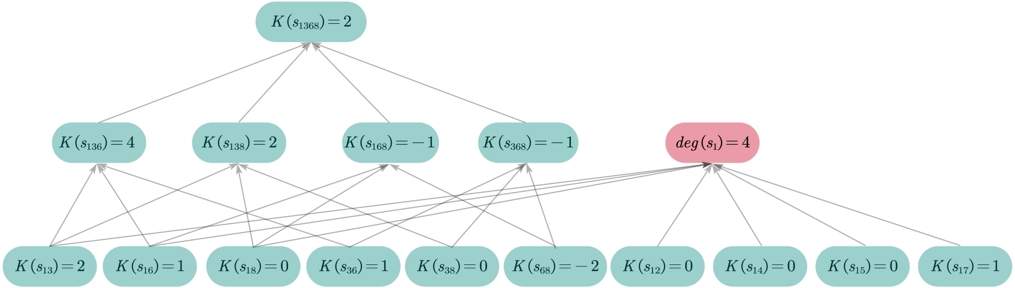

Two-particle data form the bottom layer; higher-channel nodes are linked by subset inclusion. In the factorial-rescaled variables $\widetilde{K}(A) = (|A| - 2)!K(A)$, the recursion becomes an integer sum:

$$\boxed{\widetilde{K}(A) = \sum_{B \prec A} \widetilde{K}(B)}.$$

Source: S. Li and Y. Zhang, Phys. Rev. D 113, 105006 (2026).

Discrete Backpropagation

1. Apply an integer update ΔK to a selected node at any layer.
2. When needed, distribute the update down to the two-particle data, then evaluate upward on the subset lattice.
3. If the update reaches a protected node, propagate the induced integer residual downward through other free nodes.
4. Repeat upward evaluation and backward residual propagation until all prescribed pole constraints hold exactly.

Source: S. Li and Y. Zhang, Phys. Rev. D 113, 105006 (2026), Sec. III.

Six-Point Pick-Pole Problem

Consider

$$I_6 = \frac{1}{z_{12}^2 z_{23}^2 z_{34}^2 z_{56}^2 z_{16} z_{45} z_{46} z_{15}}.$$

Its CHY integral gives

$$\frac{1}{s_{12}s_{34}s_{56}} + \frac{1}{s_{123}s_{12}s_{56}} + \frac{1}{s_{123}s_{23}s_{56}} + \frac{1}{s_{156}s_{23}s_{56}} + \frac{1}{s_{156}s_{34}s_{56}}.$$

Keep the channels $s_{12}, s_{34}, s_{56}, s_{123}$; remove s_{23} and s_{156}.

Source: S. Li and Y. Zhang, Phys. Rev. D 113, 105006 (2026), six-point example.

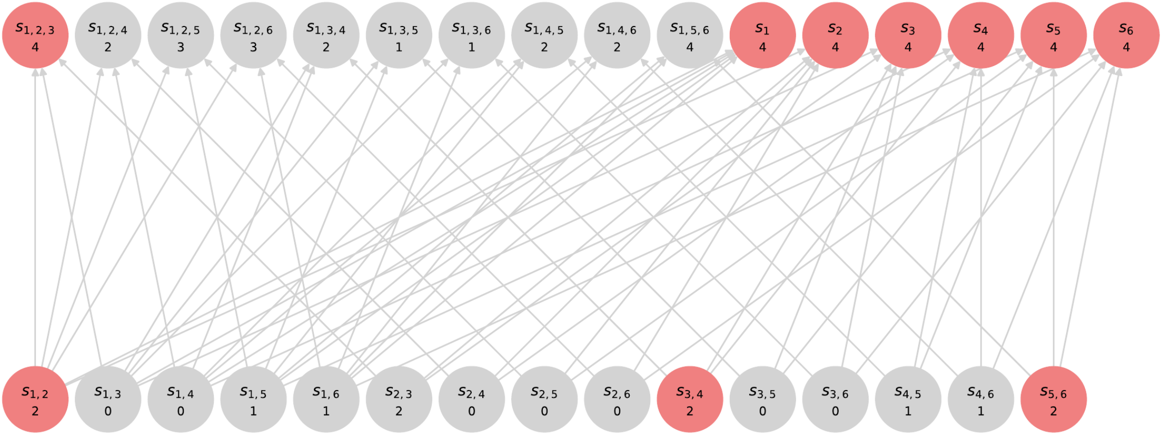

Initial state: the two-layer pole network encodes all current constraints.

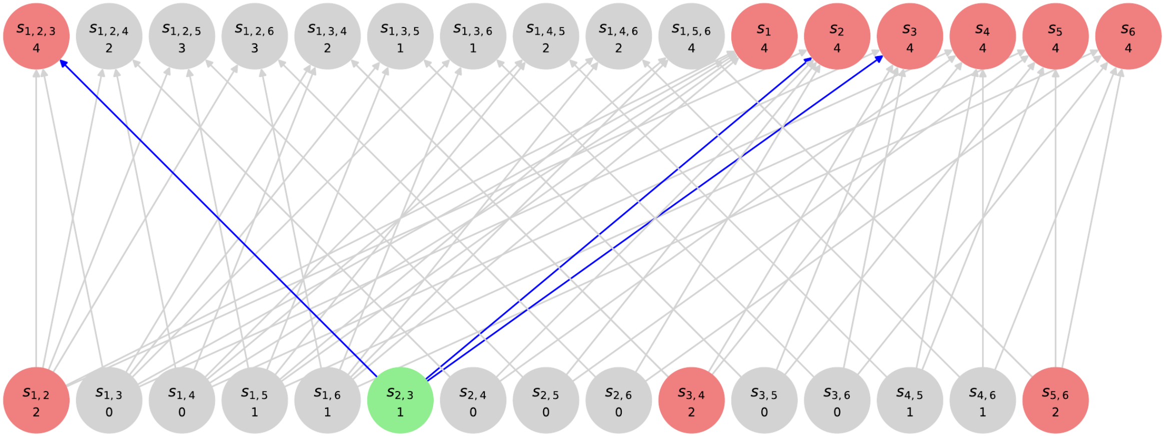

Set $\Delta K(s_{23}) = -1$; the update propagates to relevant supersets.

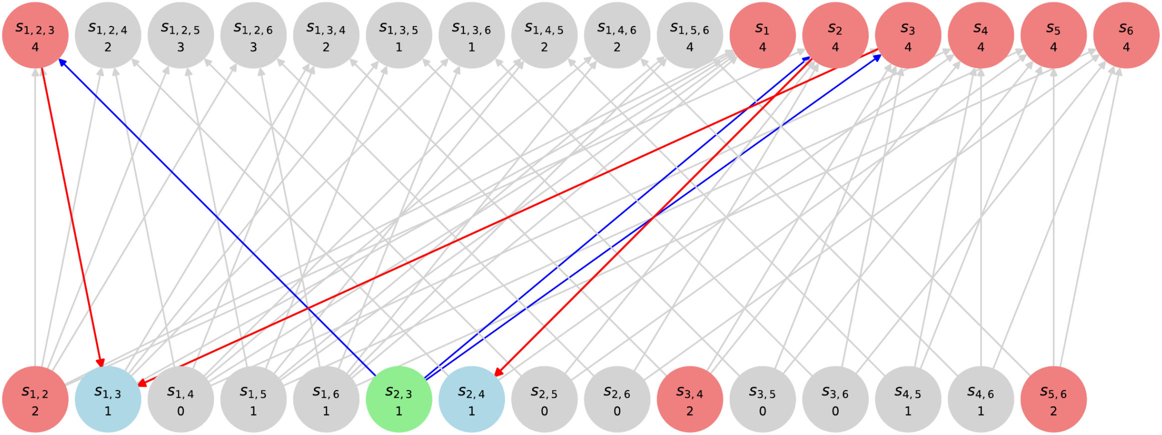

The update reaches a protected node; compensate through s_{13} and s_{24}.

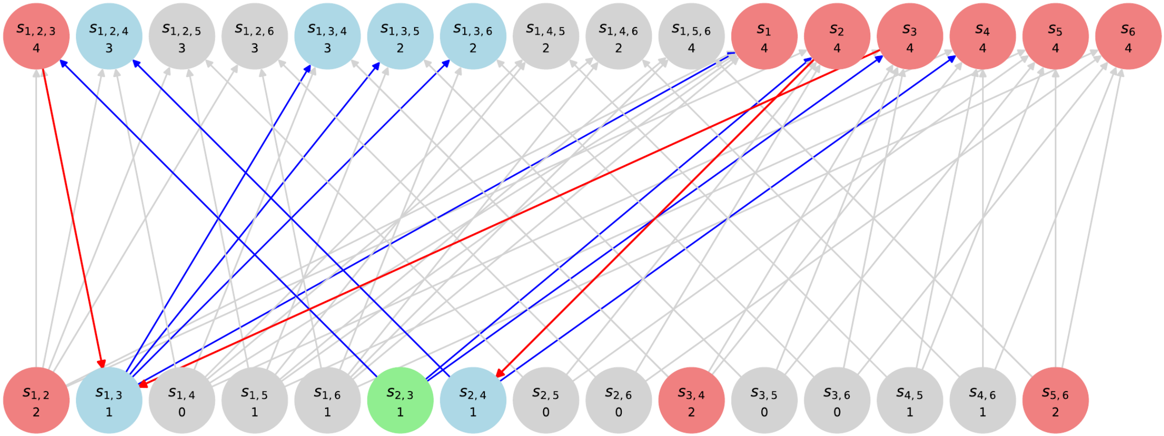

The compensating updates propagate to three-particle channels.

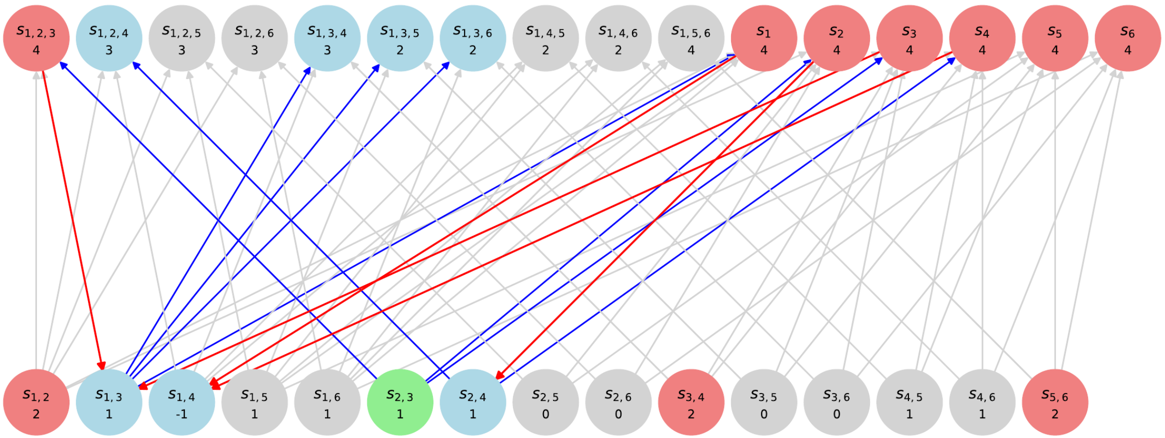

Adjust $K(s_{14})$ to restore the remaining recursion constraints.

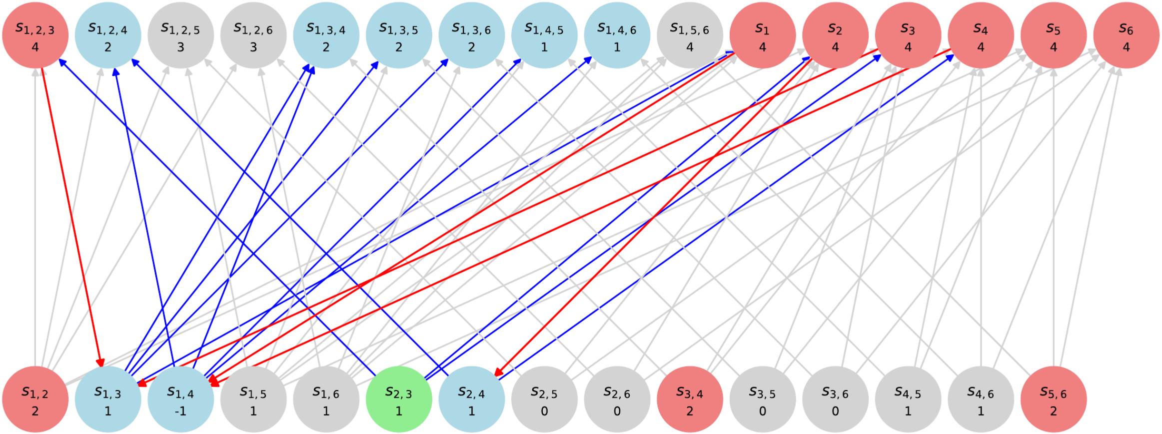

The s_{23} channel is removed; protected channels remain unchanged.

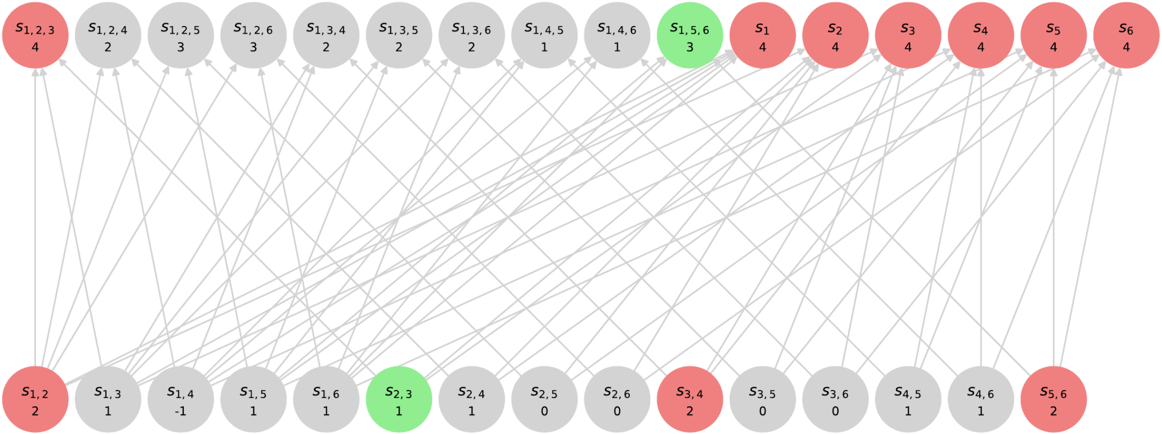

With s_{23} removed, the next channel to remove is s_{156}.

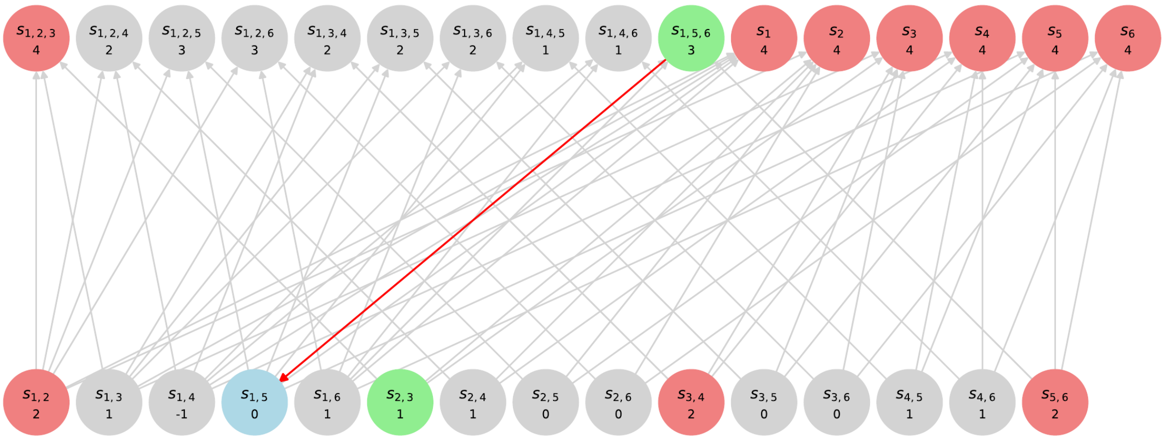

Choose the descendant s_{15} and set $\Delta K(s_{15}) = -1$.

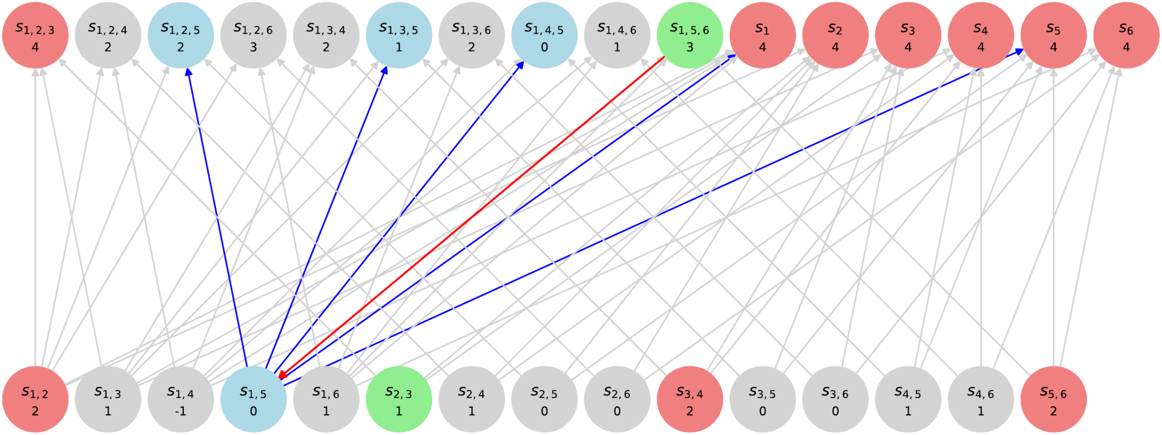

The s_{15} update reaches three-particle supersets and protected nodes.

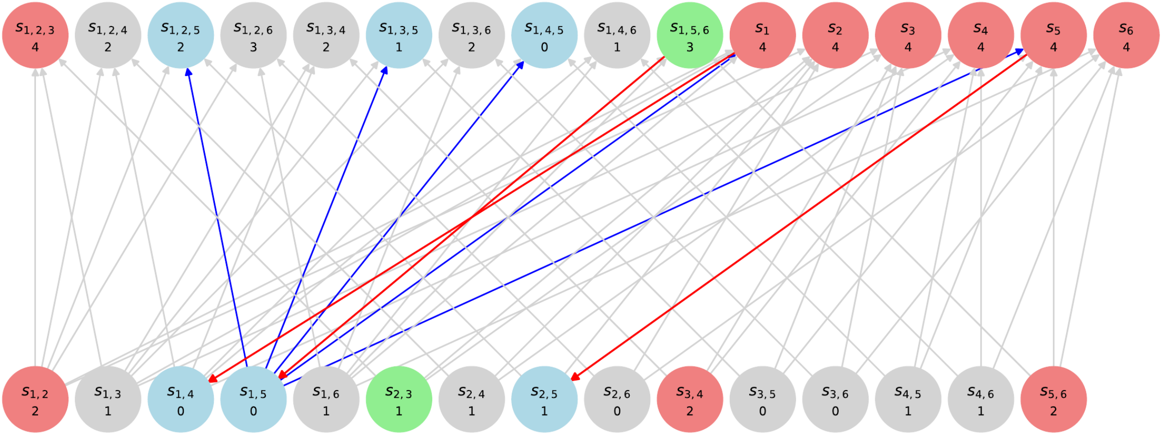

Compensate through updates to s_{14} and s_{25}.

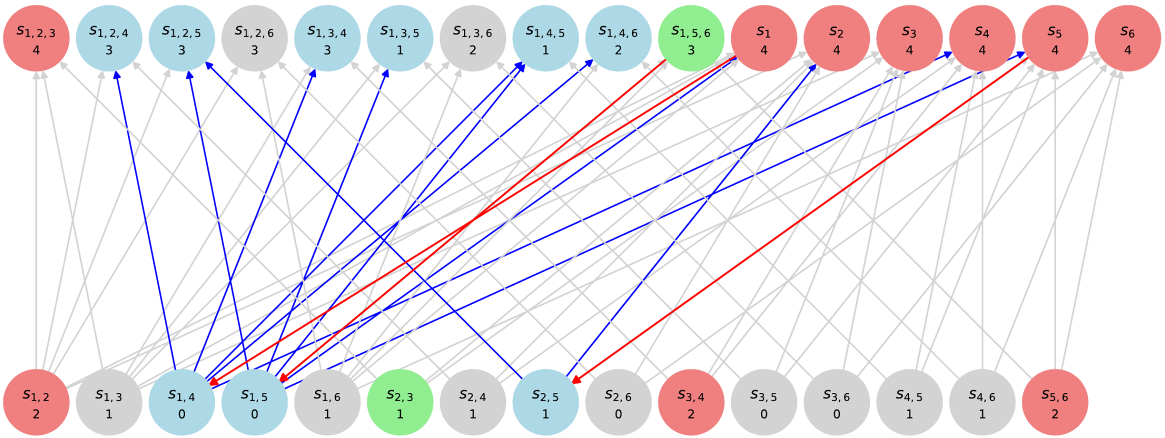

The updates propagate upward and reach the fixed nodes s_2 and s_4.

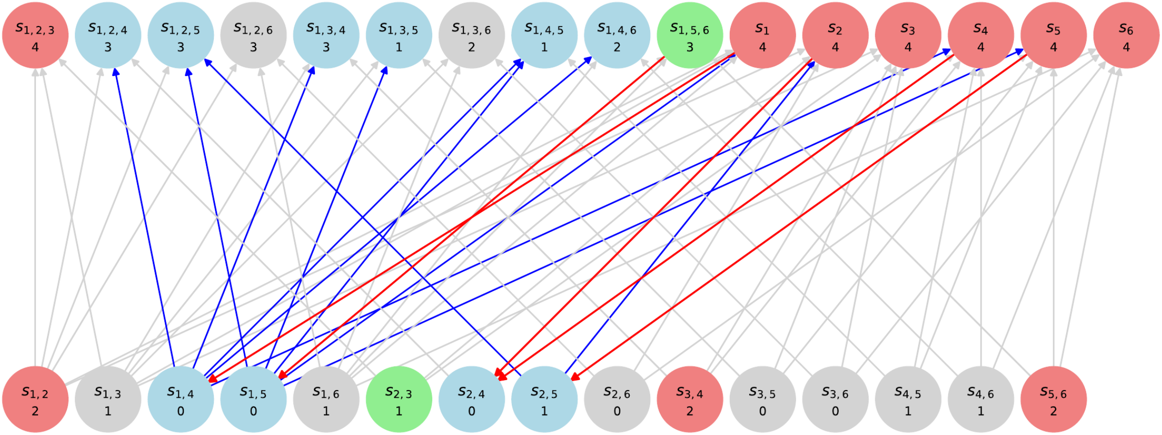

Lower $K(s_{24})$ by 1 to cancel the induced residual.

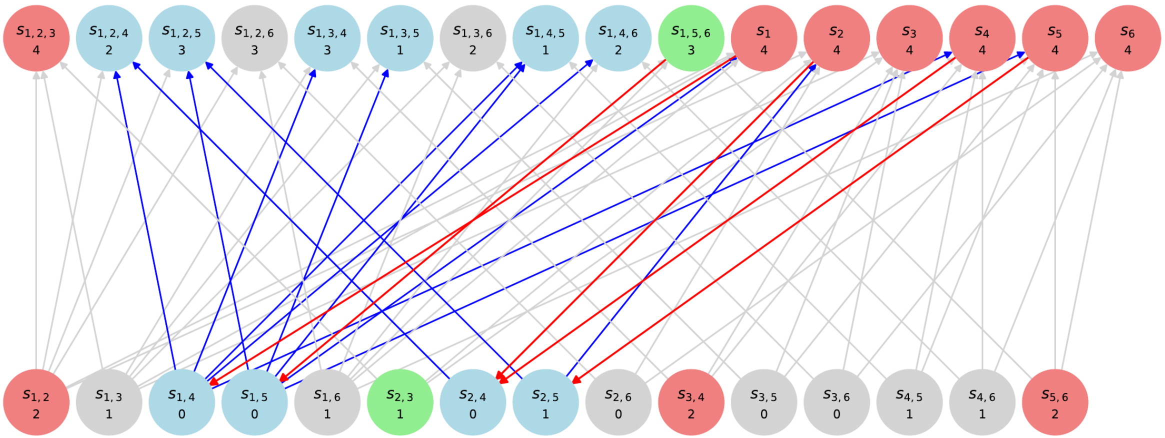

Both s_{23} and s_{156} are removed; propagation converges.

Six-Point Pick-Pole Output

Solving all constraints gives

$$I_6^* = \frac{1}{z_{12}^2 z_{13} z_{16} z_{23} z_{25} z_{34}^2 z_{45} z_{46} z_{56}^2}.$$

The corresponding amplitude is

$$\mathcal{A}_6^* = \frac{1}{s_{12} s_{34} s_{56}} + \frac{1}{s_{123} s_{12} s_{56}}.$$

This result keeps $s_{12}, s_{34}, s_{56}, s_{123}$ and removes s_{23}, s_{156}.
At higher multiplicity, the same algorithm extends to deeper subset lattices.

Source: S. Li and Y. Zhang, Phys. Rev. D 113, 105006 (2026).

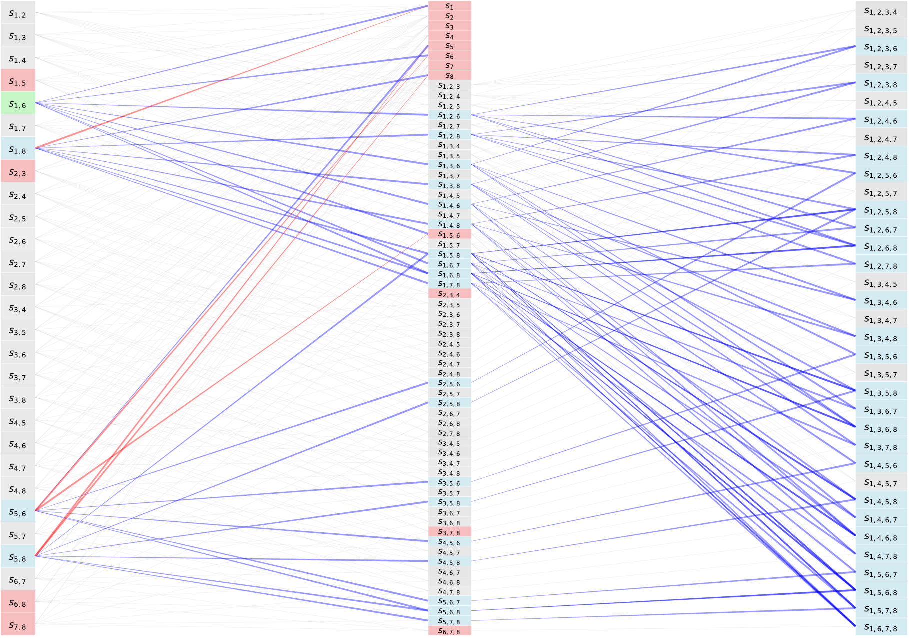

S. Li and Y. Zhang, Phys. Rev. D 113, 105006 (2026).

3: BCJ Numerators and the LLM Harness

BCJ Representations

An L-loop n-point gauge-theory amplitude can be written as a sum over oriented cubic graphs:

$$\mathcal{A}_n^{(L)} = i^L g^{n-2+2L} \sum_{g\in\Gamma_3} \int \frac{d^{LD}\ell}{(2\pi)^{LD}} \frac{1}{S_g} \frac{c_g\, n_g(\ell)}{\prod_{e\in g} D_e}.$$

Each graph carries

color factor c_g, kinematic numerator n_g, propagators D_e.

The amplitude depends on a consistent assignment across all graphs; individual numerators are representation-dependent data to be reconstructed.

Source: Z. Bern, J. J. M. Carrasco and H. Johansson, *Phys. Rev. D* 78 (2008) 085011.

Color–Kinematics Duality

Color factors obey antisymmetry and Jacobi identities:

$$c_{\bar{i}} = -c_i, \qquad c_i + c_j + c_k = 0.$$

A BCJ representation imposes the same algebraic relations on kinematic numerators:

$$\boxed{n_{\bar{i}} = -n_i, \qquad n_i + n_j + n_k = 0}.$$

Replacing $c_g \to \widetilde{n}_g$ then gives the gravity double copy:

$$\mathcal{M}_n^{(L)} \sim \sum_{g\in\Gamma_3} \int \frac{n_g \widetilde{n}_g}{S_g \prod_e D_e}.$$

The construction problem is to recover the full set $\{n_g\}$ from amplitude data and graph algebra.

Source: Z. Bern, J. J. M. Carrasco and H. Johansson, arXiv:0805.3993.

Generalized Unitarity Cuts

Unitarity reconstructs loop amplitudes from products of on-shell tree amplitudes. Generalized unitarity places more propagators on shell at once:

$$\left(\prod_{e\in C} D_e\right) \mathcal{I}_n^{(L)}\Big|_{D_e=0} = \sum_{D_s\text{-dimensional physical states}} \prod_{v\in C} \mathcal{A}_v^{\mathrm{tree}}.$$

- 1994: One-loop gauge amplitudes from cuts and collinear limits;
- 2005: Quadruple cuts isolate one-loop box coefficients;
- Loop-level construction reduces to matching on-shell tree data.

Source: Z. Bern et al., *Nucl. Phys. B* 425 (1994) 217; R. Britto, F. Cachazo and B. Feng, *Nucl. Phys. B* 725 (2005) 275.

Cut Depth Resolves Contact-Term Layers

A local one-loop five-point integrand can be expanded in inverse propagators $Y_i = D_i$:

$$I_{\rm pent}(\ell) = \frac{N_0 + \sum_i Y_i N_i + \sum_{i\leq j} Y_i Y_j N_{ij}}{Y_1 Y_2 Y_3 Y_4 Y_5}.$$

- Maximal, box, triple, and double cuts leave successively more propagators uncut;
- The maximal cut sees only N_0; lower cuts reveal N_i and N_{ij};
- For $i < j$, the result contains square-free contact terms; for $i = j$, it contains repeated-contact terms $Y_i^2 N_{ii}$;
- Each cut topology supplies distinct linear constraints.

Source: L. Mai and Y. Zhang, arXiv:2607.13412, Secs. 5–6.

BCJ Construction as a Constrained Inverse Problem

Expand the ansatz in the space allowed by locality, power counting, and graph symmetries:

$$n_g(\ell; x) = \sum_{a=1}^{1127} x_a(D_s) B_{g,a}(\ell).$$

Stacking graph identities, cut topologies, and exact kinematic samples gives

$$\boxed{A_\sigma x(D_s) = b_\sigma(D_s)}, \qquad A_\sigma \in \mathbb{Q}^{m\times 1127}.$$

Here A_σ is independent of D_s; internal-state sums enter the target $b_\sigma(D_s)$. The working specification compiles to

$$\sigma = (\text{basis},\ \text{cuts},\ \text{samples},\ \text{routing}), \qquad \mathcal{P}_\sigma = (A_\sigma, b_\sigma; S; T).$$

Source: L. Mai and Y. Zhang, arXiv:2607.13412, Eqs. (3.33)–(3.35).

Kernel and Cokernel

A cut set defines a linear map

$$A : X_\sigma \longrightarrow Y_\sigma, \qquad x \longmapsto Ax.$$

Kernel in parameter space:

$$\ker A = \{\delta x \in X_\sigma : A\delta x = 0\}, \qquad A^{-1}(b) = x_p + \ker A \quad (b \in \operatorname{im} A).$$

It records numerator deformations invisible to the cuts; $\ker A \neq \{0\}$ means the solution is non-unique.

Cokernel in target space:

$$\operatorname{coker} A = Y_\sigma / \operatorname{im} A, \qquad [b]_A := b + \operatorname{im} A.$$

$$Ax = b \quad \Longleftrightarrow \quad b \in \operatorname{im} A \quad \Longleftrightarrow \quad [b]_A = 0 \ \text{ in } \operatorname{coker} A.$$

Thus $[b]_A$ is the target obstruction: it vanishes exactly when the target is compatible with the ansatz.

Adding Cuts: Shrink the Kernel, Test the Cokernel

Add a set of cuts ΔC to the cut set C:

$$A_{C'} = \begin{pmatrix} A_C \\ R_{\Delta C} \end{pmatrix} : X_\sigma \longrightarrow Y_C \oplus Y_{\Delta C}, \qquad C' = C \cup \Delta C.$$

Kernel: Fewer Blind Directions

$$\ker A_{C'} = \ker A_C \cap \ker R_{\Delta C} \subseteq \ker A_C.$$

New cuts resolve previously invisible directions.

Cokernel: Target Consistency

$$\operatorname{coker} A_{C'} = \frac{Y_C \oplus Y_{\Delta C}}{\operatorname{im} A_{C'}},$$

$$A_{C'} x = b_{C'} \quad \Longleftrightarrow \quad [b_{C'}]_{A_{C'}} = 0.$$

Source: L. Mai and Y. Zhang, arXiv:2607.13412, Eqs. (1.6)–(1.7).

The Balance-Beam Mechanism

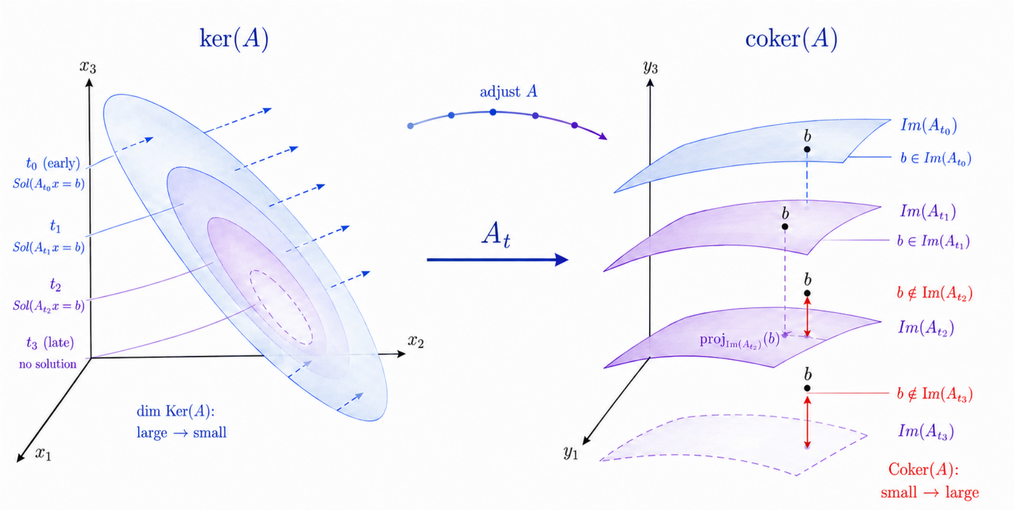

BCJ Computation Graph and Exact Diagnostics

Each candidate coefficient vector x passes through

$$x \xrightarrow{\text{Build}} N_{\text{master}} \xrightarrow{\text{Jac}} \{n_g\} \xrightarrow{\text{Prop}} \mathcal{I}_g \xrightarrow{\text{Cut}_C} A_C x.$$

A cut block therefore defines the measurement operator

$$\boxed{A_C = \text{Cut}_C \circ \text{Prop} \circ \text{Jac} \circ \text{Build}}.$$

After stacking all cuts and samples, the fixed backend compiles the specification and computes exact diagnostics:

$$\sigma \xrightarrow{\text{compile}} (A_\sigma, b_\sigma; S; T) \xrightarrow{\text{exact evaluation}} \left(\text{rank}\, A_\sigma, \ker A_\sigma, \text{coker}\, A_\sigma, [b_\sigma]_{A_\sigma}, S(\ker A_\sigma), \rho_T\right).$$

ρ_T contains exact residuals for held-out tests; $S(\ker A_\sigma)$ tests whether the remaining freedom changes the readout.

Source: L. Mai and Y. Zhang, arXiv:2607.13412, Eqs. (3.32)–(3.35).

LLM Interface and Harness

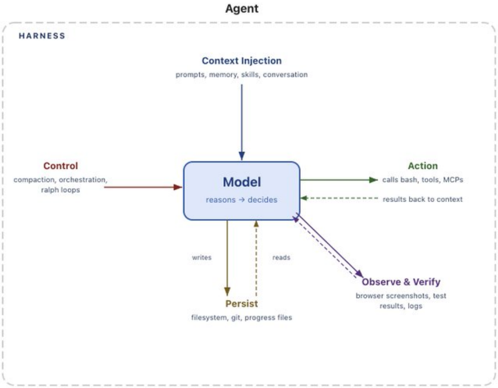

$$\{\text{Claude}, \text{GPT}, \text{DeepSeek}, \text{GLM}, \text{Qwen}, \ldots\} \xrightarrow{\text{typed proposal}} (\text{operation}, \text{parameters}).$$

$$\text{proposal} \xrightarrow{\text{fixed backend}} \text{Harness} \to \text{Compiler} \to \text{Exact Evaluator}.$$

Source: LangChain, *The Anatomy of an Agent Harness* (2026).

Exact Diagnostics Determine the Next Action

The fixed backend returns diagnostics d_t; the proposer selects one typed revision:

Incompatible Target

$$[b_t]_{A_t} \neq 0.$$

Add ansatz columns C:

$$\widetilde{A}_{t,C} := (A_t\ C), \qquad \boxed{[b_t]_{\widetilde{A}_{t,C}} = 0}.$$

Compatible but Underdetermined

$$[b_t]_{A_t} = 0, \qquad \ker A_t \neq \{0\}.$$

Add cut rows R and score the kernel reduction:

$$A_{t,R} := \begin{pmatrix} A_t \\ R \end{pmatrix}.$$

$$\boxed{g_t(R) = \dim\ker A_t - \dim\ker A_{t,R}}.$$

$$(\sigma_t, d_t) \xrightarrow{\text{propose}} \sigma_{t+1} \xrightarrow{\text{compile/evaluate/test}} d_{t+1}.$$

The specification, exact backend, and held-out tests stay fixed; only the proposal policy changes.

One-Loop Five-Gluon Case: Closing the Inverse Problem

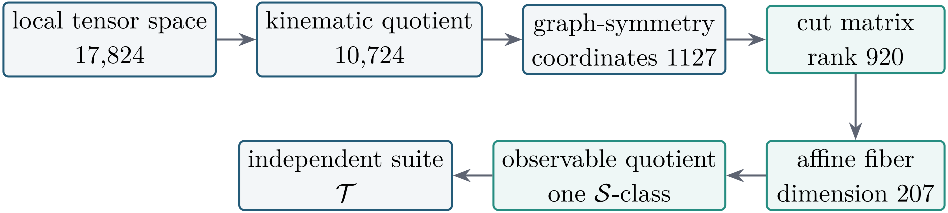

$$1127 - 920 = 207 = \dim\ker A, \qquad S|_{\ker A} = 0.$$

The full cut system leaves a 207-dimensional affine solution fiber. Since $S|_{\ker A} = 0$, every solution has the same R_{12345} color-ring readout.

Source: L. Mai and Y. Zhang, arXiv:2607.13412, Fig. 2 and Sec. 7.

The Complete Affine Solution Fiber

Exact reconstruction gives

$$A\,x(D_s) = b(D_s), \qquad x_p(D_s) = x^{(0)} + D_s x^{(1)},$$

and the complete solution family

$$\boxed{\mathcal{F}_b = x_p(D_s) + (\ker A) \otimes_{\mathbb{Q}} \mathbb{Q}(D_s)}.$$

Since A is D_s-independent, the same 207-dimensional kernel controls non-uniqueness for every D_s.

The forward-limit numerator of Cao et al. satisfies

$$x_{\mathrm{FL}} - x_p \in (\ker A) \otimes_{\mathbb{Q}} \mathbb{Q}(D_s),$$

and therefore lies in the same fiber.

Source: Q. Cao et al., *Loop-Level Double Copy Relations from Forward Limits*, arXiv:2509.25129; L. Mai and Y. Zhang, arXiv:2607.13412, Eqs. (1.8)–(1.10).

4: Summary

One Linear-Constraint Backbone

Inverse CHY with a fixed specification:

$$\mathcal{F}_{\mathrm{CHY}} = \{m \in \mathbb{Z}^N : Em = f,\ \ Gm \leq h\}.$$

The unknown is an integer-weighted graph encoding. A fixed constraint network supports discrete backpropagation through the hierarchy.

Adaptive inverse BCJ:

$$\mathcal{F}_\sigma = \{x \in \mathbb{Q}(D_s)^N : A_\sigma x = b_\sigma\} = x_p + \ker A_\sigma .$$

The unknowns include both x and the working specification σ for the coefficient space and measurements.

The first solves a fixed inverse problem; the second iteratively designs the problem itself.

Summary

1. Inverse CHY turns integrand construction into integer constraints and uses the hierarchy for discrete backpropagation;
2. BCJ numerators are constrained jointly by amplitude matching, graph Jacobi relations, locality, and generalized unitarity cuts;
3. The kernel contains cut-blind numerator directions; the cokernel records target obstructions outside the ansatz image;
4. The proposer may be a physicist, a fixed rule, or an LLM provider;
5. The harness fixes compilation, exact linear algebra, logging, and validation, keeping scientific criteria provider-independent.

Scattering amplitudes thus provide an agent testbed with exact evaluators, auditable artifacts, and held-out tests.

Thank You!

Questions & Discussion